DETECTION OF TERAHERTZ LIGHT WITH INTERSUBBAND TRANSITIONS IN SEMICONDUCTOR QUANTUM WELLS

Carey Cates, G. Brendan Serapiglia, Yuvaraj Dora, James Heyman, Jon B. Williams, Mark S. Sherwin
Center for Terahertz Science and Technology and Physics Department,
University of California Santa Barbara, Santa Barbara, CA 93106, USA

Ken Campman, Kevin D. Maranowski, Art C. Gossard
Materials Department, University of California Santa Barbara,
Santa Barbara, CA 93106, USA

William R. McGrath
NASA Jet Propulsion Laboratory, California Institute of Technology,
4800 Oak Grove Drive, Pasadena, CA 91109, USA

ABSTRACT

Intersubband transitions in semiconductor quantum well heterostructures are a promising approach for THz frequency detectors. Transistor-like devices have been fabricated from two GaAs/AlGaAs heterostructures. Detection has been observed by gate photovoltage due to optical rectification and by in-plane photoconductivity due to electron heating. These detectors have intersubband transitions that are voltage-tunable in a range of frequencies between 2.5 and 3.5THz, and have been operated at temperatures up to around 75K . These devices have been designed to include diagnostic capabilities allowing the electron intersubband dynamics to be studied.

INTRODUCTION

Semiconductor quantum well heterostructures are flexible systems that show promise for THz-frequency detectors. The operating characteristics of quantum well devices are tailorable, such as to allow operation above 20K, possibly alleviating the need to fly liquid cryogens on satellite missions. The absorption bandwidths of intersubband transitions are wide enough to allow large intermediate-frequency bandwidths for mixers but narrow enough to have a limited noise bandwidth for direct detection. In this paper we discuss results from devices that have been designed to let us directly study several detection methods and general intersubband dynamics. These devices will help us better implement more complex mixer or direct detector designs in future iterations.

DEVICE STRUCTURE

The devices were made from two doped GaAs/$Al_{0.3}Ga_{0.7}As$ quantum well heterostructures. One, ‘CC1’, has a 400Å-wide single quantum well, and another, ‘DSQB’, has a double asymmetric quantum well, with

Contact information for Carey Cates: Email: isabel@physics.ucsb.edu,

the wells of width 75Å and 85Å, separated by a 25Å barrier. Both structures yielded similar results. There are two main operational differences between the two samples. The first is that wafer CC1 has a back gate quantum well, which allows the electric field and charge density in the active area to be varied independently, while these can only be changed together in the DSQB sample. The other is the slightly different frequency ranges over which they can be tuned, 84-115cm^{-1} (2.5-3.5 THz) for the DSQB sample, and 75-160cm^{-1} (2.3-4.8 THz) for the CC1 sample. In both wafers, electrons are supplied to each quantum well by silicon DX-centers in doping layers outside the wells. The structures are designed to have the first two subbands close together in energy, to absorb in the THz frequency range, and with the next subbands sufficiently far away in energy that absorption to these states can be ignored. The doping is chosen to only populate the first subband, so the two lowest subbands can then be considered to form a two-state system.

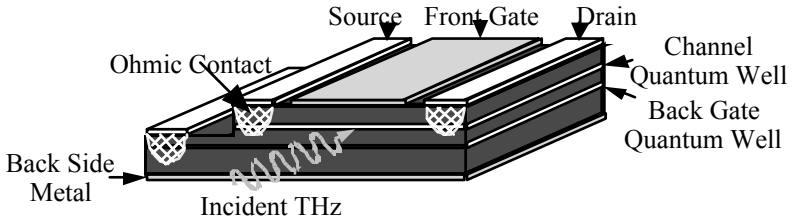

Figure 1: *Schematic of device processed from GaAs/AlGaAs quantum well heterostructure.*

The wafers were patterned into large-area transistor structures for an edge-coupling optical geometry. The devices have source and drain ohmic contacts to the channel quantum well, as shown in Figure 1. The device made from wafer CC1 also has an etched region with an ohmic contact to its back gate quantum well. All the devices have an aluminum layer that forms a Schottky contact for the front gate. There is also an aluminum layer on the back side of each device, which with the front gate, forms a waveguide. The THz light is edge-coupled into the device; it is incident on the side of the sample and travels in the waveguide between the source/drain contacts. The devices were designed to be large enough to have an easily-measurable capacitance for diagnostic purposes in studying the detection phenomena. Similarly, these devices were designed without antenna so that the bare detector performance could be studied.

MEASUREMENTS AND DISCUSSION

These devices have been designed to allow an array of electrical and optical measurements to be possible on the same device. Electrical characterization was carried out by measuring capacitance-voltage curves, and current-voltage curves over ranges of gate voltages and temperatures. The capacitance was measured between the channel quantum well layer and the front gate, which form a parallel-plate capacitor. It was measured over a range of front gate voltages from normal operating values to beyond where the channel quantum well is depleted of electrons. By integrating the capacitance from depletion to a given front gate voltage, the mobile charge present in the well at that gate voltage can be determined. The source-drain current-voltage curves can yield the in-plane resistance, which with the charge density, can be used to calculate the transport electron mobility.

Three kinds of optical measurements were performed on each sample, absorption, gate photovoltage, and in-plane photoconductivity. All optical measurements were made with the UCSB Free Electron Laser, tuned to 103 cm^{-1}. The sample transmission was measured concurrently with the in-plane photoconductivity and gate photovoltage. Varying the gate voltages changes the DC electric field across the quantum well, tuning the intersubband transition through resonant absorption of the fixed FEL frequency. By comparing the transmission of the device at operational gate voltages with transmission when the channel quantum well is depleted, the absorption due to the electrons in the quantum well alone can be determined. Reflection from the GaAs/air interface, at the edge of the sample wafer, is not significantly perturbed by the presence of the quantum wells, so the effect of changing gate voltages is negligible.

Gate Photovoltage Measurements

The gate photovoltage measurements looked at the change in capacitance induced by the THz light. The front gate and channel quantum well form a parallel-plate capacitor. The channel was grounded, and a DC voltage was applied to a resistor in series with the front gate. When the THz light was absorbed, the average position, in the heterostructure growth direction, of the electron gas changed due to the different spatial distribution of the two subbands' wavefunctions. This displacement changed the effective separation between the two plates of the capacitor. For constant bias voltage, charge was drawn to or away from the plates, drawing a current through the resistor.. The voltages at the gate and quantum well were sent to a differential preamplifier. Figure 2 shows that the gate photovoltage signal and transmission both tune through the intersubband transition resonance.

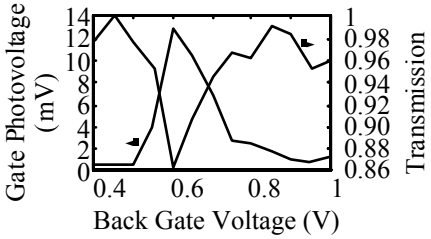

Figure 2: Gate photovoltage peak signal and relative transmission for the CC1 sample, tuning through the intersubband transition. FEL frequency is 103cm^{-1}.

Photoconductive Measurements

The photoconductive measurements looked at the resistance in the plane of the quantum wells under THz illumination. An in-plane bias current was applied between the source and drain contacts, and the voltage across these same contacts was measured. The pulsed THz light from the FEL heated the electron gas in the channel quantum well, decreasing the mobility, which resulted in a voltage pulse. In general, the photoconductive measurements were taken with the incident FEL beam attenuated such that the intersubband transition was not saturated and only electron heating was observed. Under these conditions the photosignal pulses had decay times of order a few microseconds. With higher incident FEL power, the photosignal decay times were longer than 1 ms, which we attribute to lattice heating.

The photoconductive signal was measurable over a wide device temperature range. The DSQB sample showed a photoconductive signal up to around 75K, with a maximum signal amplitude around 20K, as shown in Figure 3. A negative current was sourced, so the negative photosignal indicates an increase in resistance, as expected for electron heating. Having the peak photoconductive response around 20K offers the benefit that detector systems implementing this detection mechanism could use cooling systems without liquid cryogens, such as hydrogen sorption coolers.[1,2]

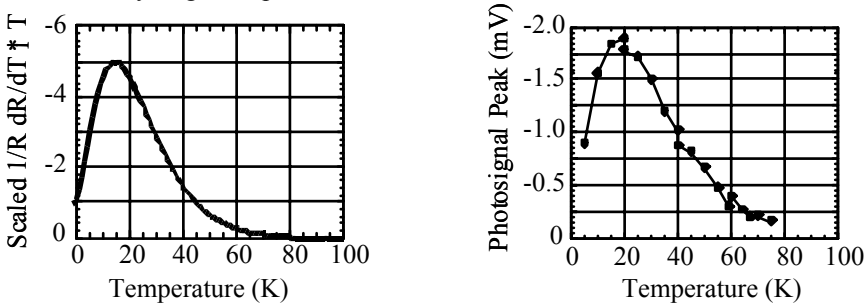

Figure 3: Left: Calculated product T_1 ($1/R_{SD}$ dR_{SD}/dT_e,), scaled by V_{SD}, device area, charge density, and K_b. Right: Photoconductive signal peak height over a range of temperatures.

We attribute the observed change in resistance is due to heating of the electron gas in the channel quantum well. In that case, the detector responsivity can be expressed in terms of the change of output voltage with electron temperature multiplied by the change in electron temperature with absorbed power,

$$R = \frac{dV}{dP_{inc}} = \eta \frac{dV}{dT_e} \frac{dT_e}{dP_{abs}} = \eta \frac{V_{SD}}{R_{SD}} \frac{dR_{SD}}{dT_e} \frac{T_1}{C_V} = \eta \frac{T_{bias} R_{SD}}{C_V} \left(T_1 \frac{-1}{\mu} \frac{d\mu}{dT_e} \right) \quad (1)$$

where η is the optical coupling, P_{inc} and P_{abs} are the incident and absorbed THz powers, T_e is the electron temperature, C_V is the specific heat of the electron gas, and T_1 is the electron energy relaxation time. V_{SD} and R_{SD} are the source-drain voltage and resistance respectively, and μ is the electron mobility. This equation assumes that the electron gas can be well described by a single electron temperature, T_e, and that the charge density in the quantum well is constant. From this equation it can be seen that for the case of an electronic bolometric response, the responsivity is proportional to the product of the energy relaxation time and the relative mobility change factor, $(1/\mu\ d\mu/dT_e)$. For a quick comparison to our data, we calculated this product for different detector temperatures. The electron energy relaxation time, T_1, was taken from measurements on another sample from the same heterostructure wafer[3] which found T_1 ranged from 1ns for T_e=10K to 10ps for T_e=50K. Electron mobility data were taken from the literature[4] for a sample with a similar low-temperature mobility (of order 10^5 cm^{-1}/Vs). Figure 3 shows the resulting product, scaled by the source-drain voltage, device area, charge density, and K_b. The scaled product is in qualitative agreement with the peak photoconductive signal as a function of temperature. Some of the factors in the responsivity vary somewhat with temperature. For example, an increase in mobile charge with increasing temperature was observed in the capacitance-voltage curves for the DSQB sample, which affects the specific heat and the source-drain resistance. These effects need to be included in a consistent manner to make the modeling quantitative, but using our initial estimates for all these factors, formula (1) does give the correct order of magnitude for the measured data. In this manner, this calculation and the observed photoconductive signal decay times are consistent with heating of the electron gas being the dominant detection mechanism for our devices.

FUTURE DIRECTIONS

We have fabricated detectors from GaAs/AlGaAs quantum well heterostructures, and demonstrated detection by gate photovoltage and by in-plane photoconductivity. The devices have been designed to accommodate several diagnostic measurements that allow the detection mechanisms and intersubband dynamics to be studied. The devices were not intended to test the ultimate sensitivity achievable with these mechanisms, but the devices do demonstrate that the relevant physical phenomena can be implemented and used in detectors at temperatures well above 4K. In this paper we have reported our initial results, and more in-depth analyses of the intersubband dynamics in these devices will be presented in future publications. In other ongoing work, we are starting to fabricate new detectors that have much smaller active regions, and also incorporate an antenna and filter circuit.

ACKNOWLEDGEMENTS

The authors would like to thank the staff of the Center for Terahertz Science and Technology at UCSB. This work was supported by NASA, ONR, NSF, NPSC (CC), and AFOSR.

REFERENCES

1. W. R. McGrath, private communication, 2000
2. C. Cates, J. B. Williams, M. S. Sherwin, K. D. Maranowski, A. C. Gossard: *Tunable Antenna-Coupled Intersubband Terahertz (TACIT) Detectors for Operation Above 4K*, Proc. Eleventh International Symposium on Space Terahertz Technology, 2000
3. J. N. Heyman, K. Unterrainer, K. Craig, B. Galdrikian, M. S. Sherwin, K. Campman, P. F. Hopkins, A. C. Gossard: *Temperature and intensity dependence of intersubband relaxation rates from photovoltage and absorption*, Physical Review Letters, **74**, (14), pp.2682-5, 1995
4. '1980' curve from Fig. 9-11, J. H. Davies: "The Physics of Low-Dimensional Semiconductors", Cambridge University Press, 1998